

## PROTEOMIC IDENTIFICATION OF PROTEINS SPECIFICALLY OXIDIZED BY INTRACEREBRAL INJECTION OF AMYLOID $\beta$ -PEPTIDE (1–42) INTO RAT BRAIN: IMPLICATIONS FOR ALZHEIMER'S DISEASE

D. BOYD-KIMBALL,<sup>a</sup> R. SULTANA,<sup>a</sup> H. FAI POON,<sup>a</sup>  
B. C. LYNN,<sup>a,b</sup> F. CASAMENTI,<sup>d</sup> G. PEPEU,<sup>d</sup> J. B. KLEIN<sup>e</sup>  
AND D. A. BUTTERFIELD<sup>a,c,\*</sup>

<sup>a</sup>Department of Chemistry, Center of Membrane Sciences, University of Kentucky, Lexington, KY, USA

<sup>b</sup>Core Proteomics Laboratory, University of Kentucky, Lexington, KY, USA

<sup>c</sup>Sanders-Brown Center on Aging, University of Kentucky, Lexington, KY, USA

<sup>d</sup>Department of Pharmacology, University of Florence, Florence, Italy

<sup>e</sup>Kidney Disease Program and Proteomics Core Laboratory, University of Louisville School of Medicine and VAMC, Louisville, KY, USA

**Abstract**—Protein oxidation has been shown to result in loss of protein function. There is increasing evidence that protein oxidation plays a role in the pathogenesis of Alzheimer's disease (AD). Amyloid  $\beta$ -peptide (1–42) [ $A\beta$ (1–42)] has been implicated as a mediator of oxidative stress in AD. Additionally,  $A\beta$ (1–42) has been shown to induce cholinergic dysfunction when injected into rat brain, a finding consistent with cholinergic deficits documented in AD. In this study, we used proteomic techniques to examine the regional *in vivo* protein oxidation induced by  $A\beta$ (1–42) injected into the nucleus basalis magnocellularis (NBM) of rat brain compared with saline-injected control at 7 days post-injection. In the cortex, we identified glutamine synthetase and tubulin  $\beta$  chain 15/ $\alpha$ , while, in the NBM, we identified 14-3-3  $\zeta$  and chaperonin 60 (HSP60) as significantly oxidized. Extensive oxidation was detected in the hippocampus where we identified 14-3-3  $\zeta$ ,  $\beta$ -synuclein, pyruvate dehydrogenase, glyceraldehyde-3-phosphate dehydrogenase, and phosphoglycerate mutase 1. The results of this study suggest that a single injection of  $A\beta$ (1–42) into NBM can have profound effects elsewhere in the brain. The results further suggest that  $A\beta$ (1–42)-induced oxidative stress in rat brain mirrors some of those proteins oxidized in AD brain and leads to oxidized proteins, which when inserted into their respective biochemical pathways yields insight into brain dysfunction that can lead to neurodegeneration in AD. © 2005 IBRO. Published by Elsevier Ltd. All rights reserved.

**Key words:** Alzheimer's disease, amyloid  $\beta$ -peptide (1–42), proteomics, oxidative stress, neurodegeneration.

\*Correspondence to: D. A. Butterfield, Department of Chemistry, Center for Membrane Sciences, and Sanders-Brown Center on Aging, 121 Chemistry-Physics Building, University of Kentucky, Lexington, KY 40506-0055, USA. Tel: +1-859-257-3184; fax: +1-859-257-5876. E-mail address: dabcsn@uky.edu (D. A. Butterfield).

**Abbreviations:**  $A\beta$ (1–42), amyloid  $\beta$ -peptide (1–42); AD, Alzheimer's disease; ChAT, choline acetyltransferase; DNP, 2,4-dinitrophenylhydrazine; DTT, dithiothreitol; GS, glutamine synthetase; HNE, 4-hydroxynonenal; HSP, heat shock protein; IA, iodoacetamide; IPG, immobilized pH gradient; NBM, nucleus basalis magnocellularis; NFT, neurofibrillary tangle; PBST, phosphate-buffered saline containing 0.01% (w/v) sodium azide and 0.2% (v/v) Tween 20.

0306-4522/05/\$30.00+0.00 © 2005 IBRO. Published by Elsevier Ltd. All rights reserved.  
doi:10.1016/j.neuroscience.2004.12.022

Cholinergic dysfunction has been described as a characteristic hallmark in Alzheimer's disease (AD), especially in the basal forebrain (Whitehouse et al., 1981; Frölich, 2002). Additionally, AD is characterized by senile plaques, neurofibrillary tangles (NFTs), and synapse loss. Senile plaques are composed primarily of fibrillary deposits of amyloid  $\beta$ -peptide (1–42) [ $A\beta$ (1–42)]. Injection of plaques isolated from AD brains into rat brain induces neuronal degradation (Frautschy et al., 1991). Likewise,  $A\beta$ (1–42) has been shown to induce cholinergic impairment when injected into rat brain (Giovannini et al., 2002).

In addition to cholinergic deficits, oxidative stress is extensive in AD.  $A\beta$ (1–42) has been shown to induce protein oxidation *in vitro* and *in vivo* (Butterfield and Lauderback, 2002; Varadarajan et al., 2000; Yatin et al., 1999; Drake et al., 2003) and, as a result, has been proposed to play a central role in the pathogenesis of AD (Selkoe, 2001; Butterfield et al., 2001; Butterfield, 2002, 2003). Protein oxidation has been shown to induce conformational changes that lead to loss of protein function (Subramaniam et al., 1997; Hensley et al., 1995; Lauderback et al., 2001). Protein oxidation is indexed by toxic metabolic intermediates known as protein carbonyls and/or 3-nitrotyrosine (Butterfield and Stadtman, 1997). Recent proteomic studies from our laboratory have identified specific protein targets of oxidative modification. These included proteins involved in energy metabolism, glutamate uptake and excitotoxicity, proteasome function, neuronal network formation, and neuronal communication (Castegna et al., 2002a,b, 2003).

In this study, we use proteomic techniques to conduct a parallel analysis between protein expression levels and protein carbonyl modification in order to identify proteins that are specifically oxidized in different regions of rat brain injected with  $A\beta$ (1–42) into the nucleus basalis magnocellularis (NBM) compared with saline-injected control, 7 days post-injection. In the NBM, we found 14-3-3  $\zeta$  and chaperonin 60 to be significantly oxidized, while in the cortex, we identified glutamine synthetase (GS) and a mixture of tubulin  $\beta$  chain 15 and  $\alpha$ -tubulin to be significantly oxidatively modified. Finally, in the hippocampus, we identified  $\beta$ -synuclein, 14-3-3  $\zeta$ , glyceraldehyde-3-phosphate dehydrogenase, pyruvate dehydrogenase, and phosphoglycerate mutase 1 as specific targets of  $A\beta$ (1–42)-induced protein oxidation. Here, we discuss the possible meaning of the oxidation of these proteins in the pathogenetic mechanisms leading to AD.

## EXPERIMENTAL PROCEDURES

### Chemicals

All chemicals were of the highest purity and were obtained from Sigma (St. Louis, MO, USA) unless otherwise noted. The OxyBlot protein oxidation detection kit was purchased from Chemicon International (Temecula, CA, USA).

### Injection of A $\beta$ (1–42) into the nucleus basalis and tissue dissection

This study was carried out with the cooperation of Professor Giancarlo Pepeu and his colleagues in the Department of Pharmacology at the University of Florence, Italy. Three-month old male Wistar rats (Harlan, Milan, Italy) weighing 230–250 g were used. The rats were housed in macrolon cages with *ad libitum* food and water and maintained on a 12-h light/dark cycle at 23 °C. All experiments were carried out according to the guidelines of the European Community's Council for Animal Experiments (86/609/EEC). All efforts were made to minimize the number of animals used and their suffering and all experiments conformed to the guidelines of the University of Florence on the ethical use of animals.

A $\beta$ (1–42) was dissolved in bidistilled water at the concentration of 4  $\mu$ g/ $\mu$ l, and the solution kept at room temperature for 3 days before use. One microliter of the solution was injected by means of a Hamilton microsyringe (Reno, NV, USA) into the right NBM under sodium pentobarbital (45 mg/kg i.p.) anesthesia at the stereotaxic coordinates: AP=−0.2, L=−2.8, from Bregma and H=7 from the dura (Paxinos and Watson, 1998). Control rats were injected with 1  $\mu$ l of saline solution.

Seven days after injection, the rats were killed by decapitation. The brains were rapidly removed and quickly dissected on ice and the brain samples were stored at −80 °C. The entire right hippocampus was taken and the right front cortex, and NBM were dissected at the following approximate coordinates (from Bregma): frontal cortex, AP=from +2.2 to +4.70 mm and L=from 0 to +2.5 mm; NBM, AP=from −0.4 to 1.80 mm and L=+1.5–3.0 mm.

### Sample preparation

Samples were homogenized by sonication in lysis buffer [10 mM HEPES pH 7.4 containing 137 mM NaCl, 4.6 mM KCl, 1.1 mM KH<sub>2</sub>PO<sub>4</sub>, 0.6 mM MgSO<sub>4</sub>, and protease inhibitors: leupeptin (0.5  $\mu$ g/ml), pepstatin (0.7  $\mu$ g/ml), type IIS soybean trypsin inhibitor (0.5  $\mu$ g/ml), and PMSF (40  $\mu$ g/ml)] and protein concentration was estimated by the Pierce BCA method. Protein (250  $\mu$ g) was aliquoted from each sample and were incubated at room temperature for 30 min in four volumes of 10 mM 2,4-dinitrophenylhydrazine in 2 M HCl for protein carbonyl derivatization/oxyblots or 2 M HCl for gel maps and mass spectrometry analysis, according to the method of Levine et al. (1994). Proteins were precipitated by addition of ice-cold 100% trichloroacetic acid to a final concentration of 15% for 10 min on ice. Precipitates were centrifuged for 2 min at 14,000 $\times$ g at 4 °C. The pellet was retained and washed with 500  $\mu$ l of 1:1 (v/v) ethyl acetate/ethanol three times. The final pellet was dissolved in rehydration buffer containing 8 M urea, 2 M thiourea, 2% CHAPS, 0.2% (v/v) biolytes, 50 mM dithiothreitol (DTT), and Bromophenol Blue. Samples were sonicated in rehydration buffer on ice three times for 20 s intervals.

### Immunoprecipitation

Hippocampi from saline- and A $\beta$ (1–42)-intracerebral injected rats were homogenized in lysis buffer and then 250  $\mu$ g of protein was incubated with mouse monoclonal anti-GADPH (5  $\mu$ g; Stressgen Biotech, Victoria, BC, Canada) for 12 h at 4 °C followed by protein

A-sepharose incubation for 1 h at 4 °C. Immunoprecipitated proteins were pelleted at 1500 $\times$ g, and the supernatant was used to confirm the identification of GADPH as one of the A $\beta$ (1–42)-induced oxidized proteins.

### Two-dimensional gel electrophoresis and Western blotting

Two-dimensional polyacrylamide gel electrophoresis was performed with a Bio-Rad system using 110-mm pH 3–10 immobilized pH gradients (IPG) strips and Criterion 8–16% linear gradient resolving gels. IPG strips were actively rehydrated at 50 V 20 °C overnight. Protein (250  $\mu$ g per strip) was loaded during active rehydration. Isoelectric focusing of strips loaded with protein via active rehydration was performed at 20 °C as follows: 300 V for 2 h linear gradient, 500 V 2 h linear gradient, 1000 V 2 h linear gradient, 8000 V 8 h linear gradient, 8000 V 10 h rapid gradient. Gel strips were equilibrated for 10 min prior to second-dimension separation in 0.375 M Tris–HCl pH 8.8 containing 6 M urea (Bio-Rad, Hercules, CA, USA), 2% (w/v) sodium dodecyl sulfate, 20% (v/v) glycerol, and 0.5% DTT (Bio-Rad) followed by re-equilibration for 10 min in the same buffer containing 4.5% iodoacetamide (IA; Bio-Rad) in place of DTT. Control and A $\beta$  strips were placed on the Criterion gels, prestained molecular standards were applied, and electrophoresis was performed at 200 V for 65 min.

### SYPRO Ruby staining

Gels were fixed in a solution containing 10% (v/v) methanol, 7% (v/v) acetic acid for 20 min and stained overnight at room temperature with agitation in 50 ml of SYPRO Ruby gel stain (Bio-Rad).

### Immunochemical detection

For immunoblotting analysis, electrophoresis was performed as stated previously and gels were transferred to a nitrocellulose membrane. The membranes were blocked with 3% bovine serum albumin in phosphate-buffered saline containing 0.01% (w/v) sodium azide and 0.2% (v/v) Tween 20 (PBST) overnight at 4 °C. The membranes were incubated with anti-2,4-dinitrophenylhydrazine (DNP) polyclonal antibody (1:100) or anti-14-3-3  $\zeta$  monoclonal antibody (1:1000) for 2 h in PBST for 2 h at room temperature with rocking. Following completion of the primary antibody incubation, the membranes were washed three times in PBST for 5 min each. An anti-rabbit IgG or anti-mouse alkaline phosphatase secondary antibody was diluted 1:3000 in PBST and incubated with the membranes for 2 h at room temperature. The membranes were washed in PBST three times for 5 min and developed using Sigmafast Tablets (BCIP/NBT substrate). Blots were dried and scanned with Adobe Photoshop.

### In-gel digestion

Samples were prepared according to the method described by Thongboonkerd et al. (2002). Briefly, the protein spots were cut and removed from the gel with a clean razor blade. The gel pieces were placed into individual, clean 1.5 ml microcentrifuge tubes and kept overnight at −20 °C. The gel pieces were thawed and washed with 0.1 M ammonium bicarbonate (NH<sub>4</sub>HCO<sub>3</sub>) for 15 min at room temperature. Acetonitrile was added to the gel pieces and incubated for an additional 15 min. The liquid was removed and the gel pieces were allowed to dry. The gel pieces were rehydrated with 20 mM DTT (Bio-Rad) in 0.1 M NH<sub>4</sub>HCO<sub>3</sub> and incubated for 45 min at 56 °C. The DTT was removed and replaced with 55 mM IA (Bio-Rad) in 0.1 M NH<sub>4</sub>HCO<sub>3</sub> for 30 min in the dark at room temperature. The liquid was drawn off and the gel pieces were incubated with 50 mM NH<sub>4</sub>HCO<sub>3</sub> at room temperature for 15 min. Acetonitrile was added to the gel pieces for 15 min at room

temperature. All solvents were removed and the gel pieces were allowed to dry for 30 min. The gel pieces were rehydrated with addition of a minimal volume of 20 ng/ $\mu$ l modified trypsin in 50 mM  $\text{NH}_4\text{HCO}_3$ . The gel pieces were chopped and incubated with shaking overnight (approximately 18 h) at 37 °C.

### Analysis of gel images

The analysis of the gel maps and membranes to compare protein expression and carbonyl immunoreactivity content between control and A $\beta$  treated samples was performed with PDQuest software (Bio-Rad). Images from SYPRO Ruby-stained gels, used to measure protein content, were obtained using a UV transilluminator ( $\lambda_{\text{ex}}$ =470 nm,  $\lambda_{\text{em}}$ =618 nm; Molecular Dynamics, Sunnyvale, CA, USA). Oxyblots, used to measure carbonyl immunoreactivity, were scanned with a Microtek Scanmaker 4900.

### Mass spectrometry

For this study all mass spectra were recorded at the University of Kentucky Mass Spectrometry Facility (UKMSF). A Bruker Autoflex MALDI TOF (matrix assisted laser desorption-time of flight) mass spectrometer (Bruker Daltonics, Billerica, MA, USA) operated in the reflection mode was used to generate peptide mass fingerprints. Peptides resulting from in-gel digestion were analyzed on a 384 position, 600  $\mu$ m Anchor-Chip Target (Bruker Daltonics, Bremen, Germany) and prepared according to AnchorChip recommendations (AnchorChip Technology, Rev. 2; Bruker Daltonics, Bremen, Germany). Briefly, 1  $\mu$ l of digestate was mixed with 1  $\mu$ l of  $\alpha$ -cyano-4-hydroxycinnamic acid (0.3 mg/ml in ethanol:acetone, 2:1 ratio) directly on the target and allowed to dry at room temperature. The sample spot was washed with 1  $\mu$ l of 1% TFA solution for approximately 60 s. The TFA droplet was gently blown off the sample spot with compressed air. The resulting diffuse sample spot was recrystallized (refocused) using 1  $\mu$ l of a solution of ethanol:acetone:0.1% TFA (6:3:1 ratio). Reported spectra are a summation of 100 laser shots. External calibration of the mass axis was used for acquisition and internal calibration using either trypsin autolysis ions or matrix clusters was applied post acquisition for accurate mass determination.

### Analysis of peptide sequences

Peptide mass fingerprinting was used to identify proteins from tryptic peptide fragments by utilizing the MASCOT search engine (www.matrixscience.com) based on the entire NCBI and SwissProt protein databases. Database searches were conducted allowing for up to one missed trypsin cleavage and using the assumption that the peptides were monoisotopic, oxidized at methionine residues, and carbamidomethylated at cysteine residues. Mass tolerance of 150 ppm/g was the window of error allowed for matching the peptide mass values. Probability-based MOWSE scores were estimated by comparison of search results against estimated random match population and were reported as  $-10 \times \log_{10}(P)$ , where  $P$  is the probability that the identification of the protein is not correct. MOWSE scores greater than 47 were considered to be significant ( $P < 0.05$ ). All protein identifications were in the expected size and pI range based on position in the gel.

### Statistical analysis

Statistical comparison of carbonyl levels of proteins, matched with anti-DNP positive spots on 2D-oxyblots from brain regions isolated from rats injected with A $\beta$ (1–42) and brain regions isolated from rats injected with saline, was performed using ANOVA.  $P$  values of  $< 0.05$  were considered to be significant.

## RESULTS

Comparison of protein oxidation levels in brain regions of rats injected with A $\beta$ (1–42) and brain regions of control rats injected with saline was carried out by first identifying carbonylated proteins via anti-DNP immunochemical development of proteins transferred to a nitrocellulose membrane, or 2D-oxyblot analysis (cortex: Fig. 1B; hippocampus: Fig. 3B; NBM: Fig. 5B). Individual protein spots were matched between the 2D-PAGE maps and the 2D-oxyblots and the carbonyl immunoreactivity of each spot was

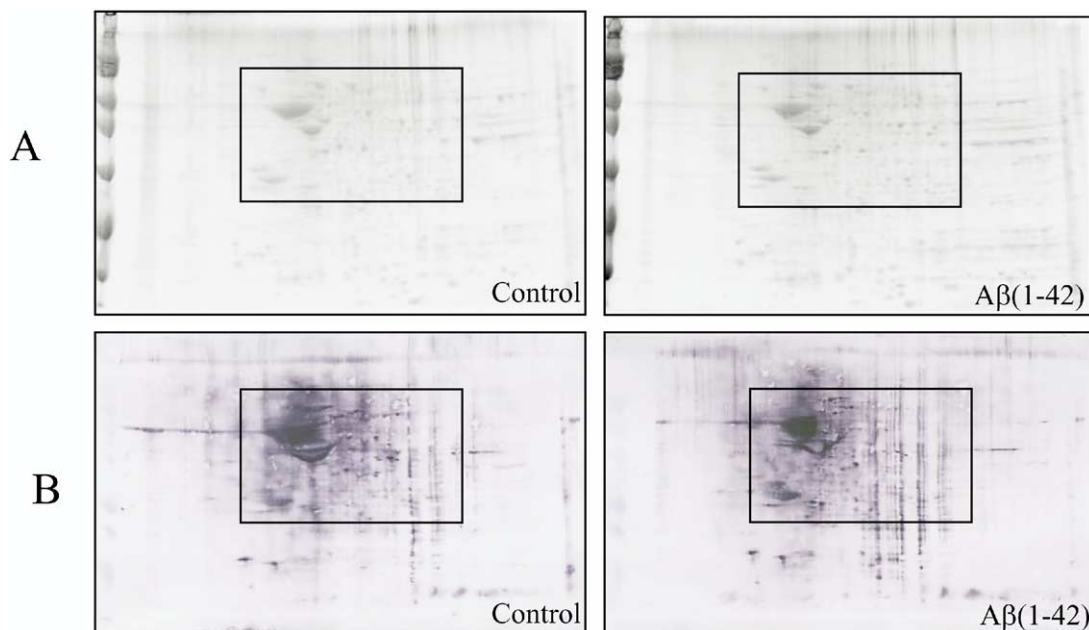
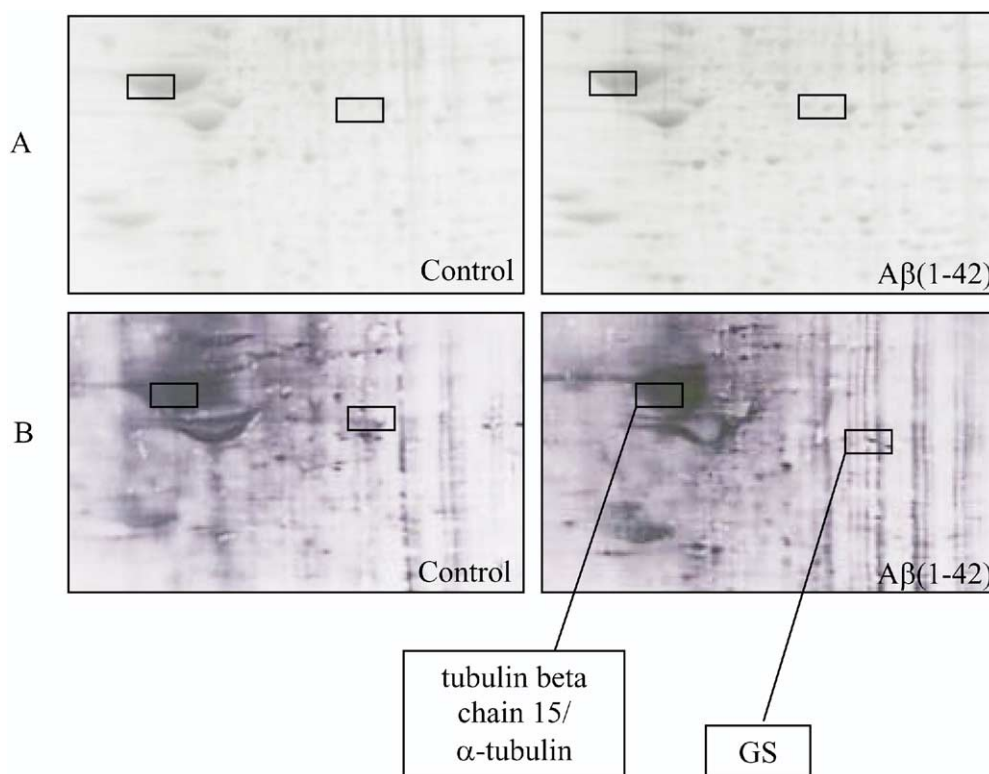


**Fig. 1.** Sypro Ruby-stained 2D gels (A) and 2D-oxyblots (B) from cortex isolated from saline-(control) and A $\beta$ (1–42) injected rats. The boxes represent the area enlarged in Fig. 2.

normalized to the protein content in the 2D-PAGE (cortex: Fig. 1A; hippocampus: Fig. 3A; NBM: Fig. 5A). In this study we confirm previous reports that in brain in oxidative stress conditions, many, but not all, individual proteins exhibit carbonyl immunoreactivity (Castegna et al., 2002a,b, 2003, 2004). Others, using proteomics, confirmed our findings (Castegna et al., 2002a) that ubiquitin carboxyl-terminal hydrolase L-1 is an oxidized protein in AD brain (Choi et al., 2004).

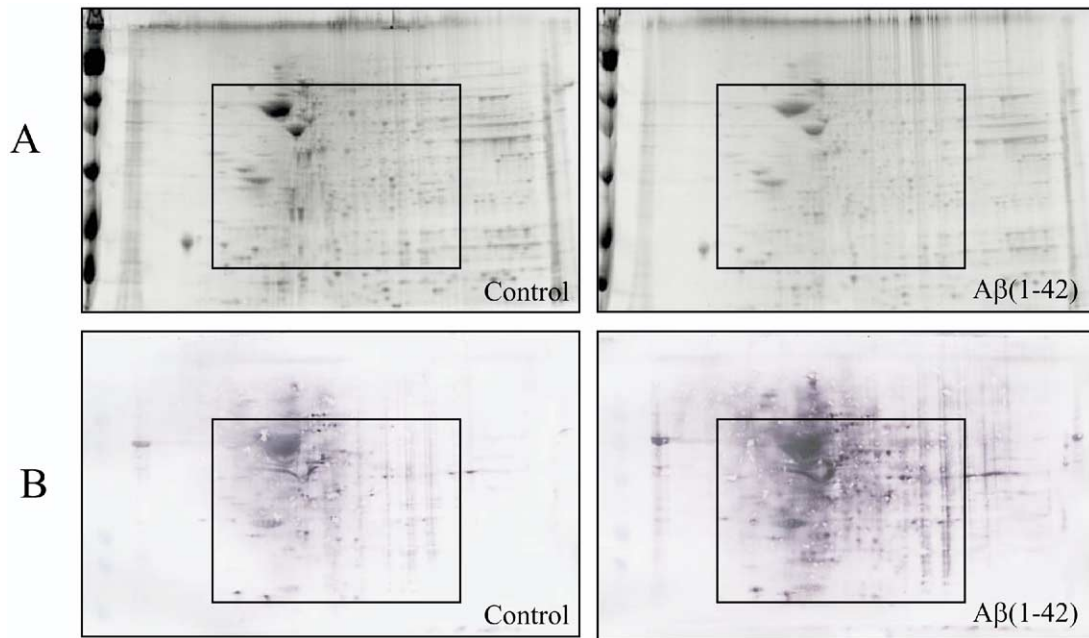
Mass spectrometry analysis allowed for the identification of protein spots from different brain regions that were found to be increasingly carbonylated following A $\beta$ (1–42) injection to the rat basal forebrain. In the cortex, GS and a mixture of tubulin  $\beta$  chain 15 and  $\alpha$ -tubulin were found exhibit a significant increase in protein carbonylation (Fig. 2). In the hippocampus,  $\beta$ -synuclein, 14-3-3  $\zeta$ , glyceraldehyde-3-phosphate dehydrogenase, pyruvate dehydrogenase, phosphoglycerate mutase 1, and phosphoglycerate mutase 2 were found to be significantly increased in protein oxidation (Fig. 4). Finally, in the NBM 14-3-3  $\zeta$  and chaperonin 60 (HSP 60) were found to be significantly oxidatively modified (Fig. 6). Using MASCOT, the probability based MOWSE score was 73 for GS, with eight of 29 peptide matches and 17% sequence coverage; 226 for the mixture of tubulin  $\beta$  chain 15 (MOWSE score 146), with 24/75 peptide matches and 50% sequence coverage and  $\alpha$ -tubulin (MOWSE score 70), with 13/75 peptide matches and 41% sequence coverage; 99 for  $\beta$ -synuclein, with six of 13 peptide matches and 43% sequence coverage; 152

for 14-3-3  $\zeta$ , with 14/29 peptide matches and 44% sequence coverage; 144 for glyceraldehyde-3-phosphate dehydrogenase, with 14/44 peptide matches and 42% sequence coverage; 64 for pyruvate dehydrogenase, with eight of 27 peptide matches and 16% sequence coverage; 132 for phosphoglycerate mutase 1, with 13/43 peptide matches and 62% sequence coverage; 130 for phosphoglycerate mutase 1, with 11/27 peptide matches and 57% sequence coverage; 104 for 14-3-3  $\zeta$ , with 10/28 peptide matches and 32% sequence coverage; and 67 for chaperonin 60, with 9/25 peptide matches and 19% sequence coverage. The increase in carbonylation compared with control was significant for GS ( $839 \pm 301\%$  control,  $P < 0.04$ ) and tubulin ( $201,102 \pm 35,678\%$  control,  $P < 0.02$ ) in the cortex, 14-3-3  $\zeta$  ( $866 \pm 127\%$  control,  $P < 0.001$ ) and chaperonin 60 ( $1605 \pm 425\%$  control,  $P < 0.006$ ) in the NBM, and  $\beta$ -synuclein ( $112 \pm 22\%$  control,  $P < 0.04$ ), 14-3-3  $\zeta$  ( $290 \pm 68\%$  control,  $P < 0.03$ ), glyceraldehyde-3-phosphate dehydrogenase ( $1463 \pm 548\%$  control,  $P < 0.03$ ), pyruvate dehydrogenase ( $1783 \pm 493\%$  control,  $P < 0.007$ ), phosphoglycerate mutase 1 ( $1014 \pm 258\%$  control,  $P < 0.009$ ), and phosphoglycerate mutase 1 ( $1147 \pm 317\%$  control,  $P < 0.04$ ). Note that two spots were identified as phosphoglycerate mutase 1. It is likely that both spots represent the same protein, but may represent different phosphorylation states resulting in the shift in pI between the spots (Fig. 4). Information about the proteins identified in this study is summarized in Table 1.



**Fig. 2.** Enlargements of 2D gel (A) and 2D oxyblot (B) images show the position of protein spots and carbonyl immunoreactivity, respectively. The 2D-oxyblot of cortex isolated from A $\beta$ (1–42)-injected rats is labeled with the proteins identified in this study.

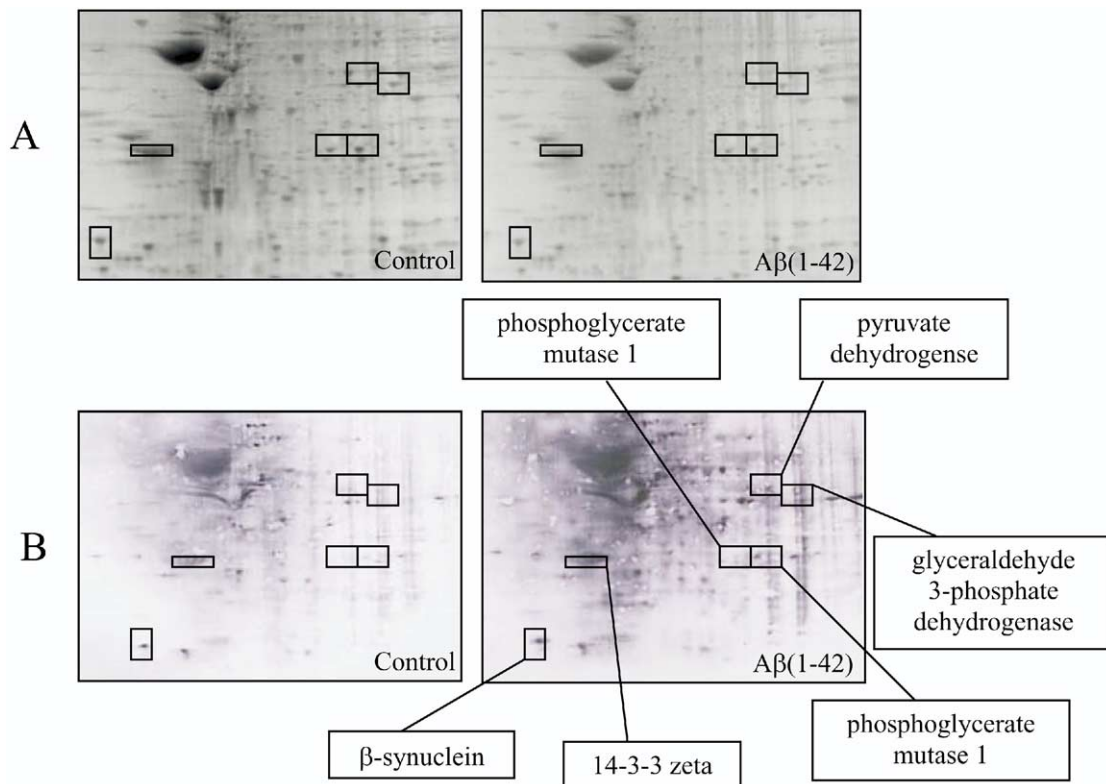




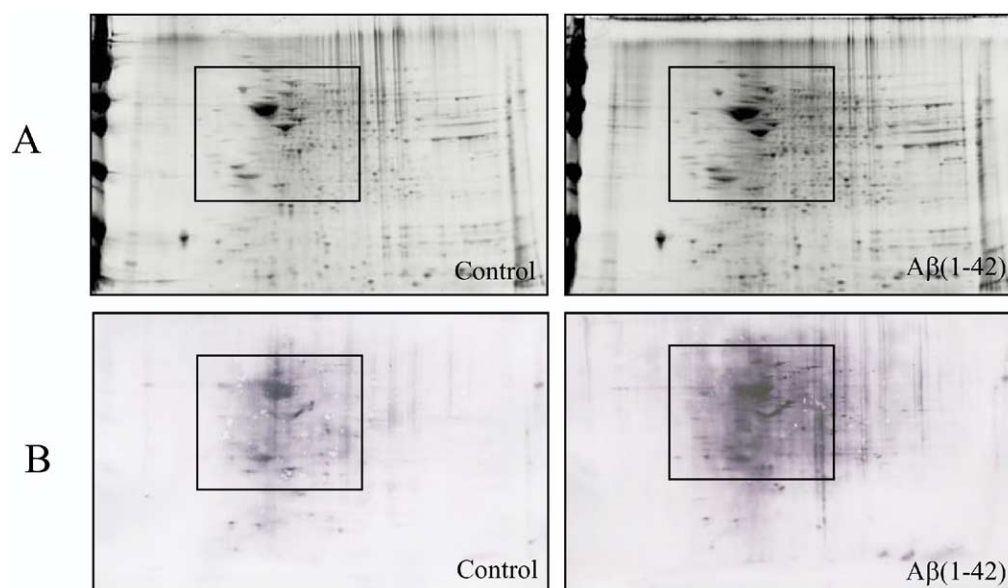
**Fig. 3.** Sypro Ruby-stained 2D gels (A) and 2D-oxyblots (B) from hippocampus isolated from saline- (control) and A $\beta$ (1–42)-injected rats. The boxes represent the area enlarged in Fig. 4.

Fig. 7a and b showed ponceau-stained and anti-14-3-3  $\zeta$ -probed blots. The 14-3-3  $\zeta$ -probed blot showed a single spot at the same position as reported for the oxidized

14-3-3  $\zeta$  protein in Fig. 4 based on mass spectrometry data. In addition, Fig. 8a and c shows the gel and Western blot from the sample immunoprecipitated with anti-GADPH



**Fig. 4.** Enlargements of 2D gel (A) and 2D oxyblot (B) images show the position of protein spots and carbonyl immunoreactivity, respectively. The 2D-oxyblot of hippocampus isolated from A $\beta$ (1–42)-injected rats is labeled with the proteins identified in this study.



**Fig. 5.** Sypro Ruby-stained 2D gels (A) and 2D-oxyblots (B) from NBM isolated from saline- (control) and A $\beta$ (1–42)-injected rats. The boxes represent the area enlarged in Fig. 6.

antibody. No spot corresponding to GADPH was detected on both the gel and blot, confirming the correct identification of these proteins based on mass data.

## DISCUSSION

Previous studies have shown that A $\beta$ (1–42) induces protein oxidation *in vitro* in synaptosomal preparations and neuronal cultures, and *in vivo* in *Caenorhabditis elegans* expressing A $\beta$ (1–42) (Yatin et al., 1999, 2000; Varadarajan et al., 2000; Drake et al., 2003). Knock-in mice with mutant human genes for amyloid precursor protein and presenilin-1, which have increased production of human A $\beta$ (1–42), have increased protein oxidation in brain (Mo-

hammad-Abdul et al., 2004). It has also been shown that A $\beta$ (1–42) induces formation of the lipid peroxidation product 4-hydroxynonenal (HNE; Mark et al., 1997; Lauderback et al., 2001). HNE is a reactive alkenal, found to be increased in AD brain (Markesbery and Lovell, 1998), that reacts by Michael addition with protein-bound cysteine, lysine, and histidine to add carbonyl functionality (Esterbauer et al., 1991). Enzymes, such as GS, creatine kinase, and the glutamate transporter EAAT2, which have been found to have significantly decreased activity in AD brain have been shown to be oxidatively modified in AD brain (Hensley et al., 1995; Aksenov et al., 1999; Masliah et al., 1996; Lauderback et al., 2001). It is likely that the oxidative

**Table 1.** Summary of the proteins identified by proteomics to be increasingly carbonylated in brain regions isolated from rats treated *in vivo* with A $\beta$ (1–42)<sup>a</sup>

| Protein                                     | Mowse score | Peptides matched | % Coverage | % Increase carbonyls | MW            | pI        | P value |
|---|-------------|------------------|------------|----------------------|---------------|-----------|---------|
| <b>NBM</b>                                  |             |                  |            |                      |               |           |         |
| 14-3-3 $\zeta$                              | 104         | 10               | 32         | 866 $\pm$ 77         | 27,955        | 4.73      | <0.001  |
| chaperonin 60                               | 67          | 9                | 19         | 1605 $\pm$ 375       | 61,029        | 5.78      | <0.006  |
| <b>Cortex</b>                               |             |                  |            |                      |               |           |         |
| Glutamate-ammonia ligase (GS)               | 73          | 8                | 17         | 839 $\pm$ 251        | 42,240        | 6.64      | <0.04   |
| Tubulin $\beta$ chain 15/ $\alpha$ -tubulin | 146/70      | 24/13            | 50/41      | 201,102 $\pm$ 71,357 | 50,361/50,816 | 4.79/4.94 | <0.02   |
| <b>Hippocampus</b>                          |             |                  |            |                      |               |           |         |
| $\beta$ -Synuclein                          | 99          | 6                | 43         | 112 $\pm$ 45         | 14,495        | 4.48      | <0.04   |
| 14-3-3 $\zeta$                              | 152         | 14               | 44         | 390 $\pm$ 18         | 27,955        | 4.73      | <0.03   |
| Glyceraldehyde-3-phosphate dehydrogenase    | 144         | 14               | 42         | 1143 $\pm$ 408       | 36,090        | 8.14      | <0.03   |
| Pyruvate dehydrogenase (lipoamide)          | 64          | 8                | 16         | 1014 $\pm$ 208       | 43,853        | 8.35      | <0.007  |
| Phosphoglycerate mutase 1                   | 132         | 13               | 62         | 1462 $\pm$ 499       | 28,923        | 6.67**    | <0.009  |
| Phosphoglycerate mutase 1                   | 130         | 11               | 57         | 1783 $\pm$ 443       | 28,923        | 6.67**    | <0.04   |

<sup>a</sup> For each protein the carbonyl immunoreactivity/protein expression values were averaged ( $n=5$ ) and expressed as percentage control $\pm$ SEM.

\*\* pI value as reported by MASCOT search. pI of protein spots in the 2D-gel varying from one another indicating the possibility of different phosphorylation states between the two.

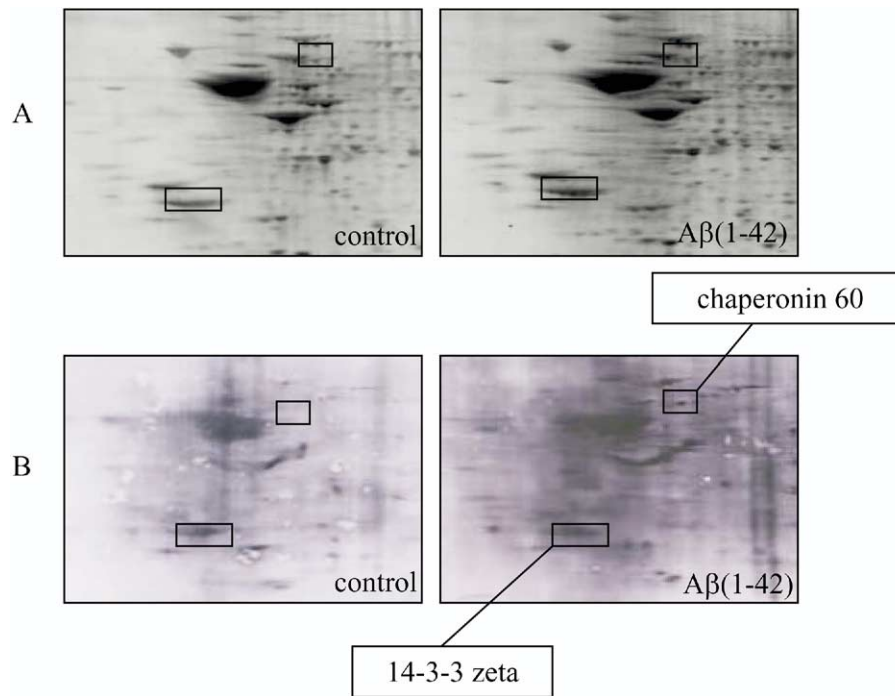


**Fig. 6.** Enlargements of 2D gel (A) and 2D oxyblot (B) images show the position of protein spots and carbonyl immunoreactivity, respectively. The 2D-oxyblot of NBM isolated from A $\beta$ (1–42)-injected rats is labeled with the proteins identified in this study.

modification of these proteins is responsible for the loss of function of these proteins. For example, HNE is known to alter the physical state of synaptosomal proteins (Subramaniam et al., 1997). Consequently, it is likely that proteins found to be oxidized in the cortex, NBM, and hippocampus of rat brain injected with A $\beta$ (1–42) have undergone a conformational change in structure which alters the function of these proteins. The proteins identified in this study are associated with cellular structure, signal transduction, glycolysis and energy metabolism, excitotoxicity, and stress responses. Altered function of these proteins could play a role in the neurodegeneration exhibited in AD.

14-3-3  $\zeta$  was found to be oxidized in both the NBM and the hippocampus. 14-3-3  $\zeta$  is a cytosolic protein that is part of a 14-3-3 protein family which are highly expressed in the

brain (Takahashi, 2003; Dougherty and Morrison, 2004). 14-3-3 proteins are involved in a number of cellular functions including signal transduction, protein trafficking and metabolism (Dougherty and Morrison, 2004). Once bound to a target protein, 14-3-3 can regulate the target protein in a variety of ways including acting as a bridge (adaptor/scaffold) between two target proteins, altering (either increase or inhibit) the intrinsic catalytic activity of the target protein, and can protect the target protein from proteolysis and dephosphorylation (Takahashi, 2003).

Levels of 14-3-3 proteins are increased in AD brain (Fountoulakis et al., 1999), found in AD CSF (Burkhard et al., 2001) and are associated with neurofibrillary tangles (NFT) in AD brain (Layfield et al., 1996). NFTs are a hallmark of AD composed of paired helical filaments con-



**Fig. 7.** Western blot showing ponceau-stained (a) and anti-14-3-3  $\zeta$ -probed blots (b). Box represents the location of 14-3-3  $\zeta$  on the blots.

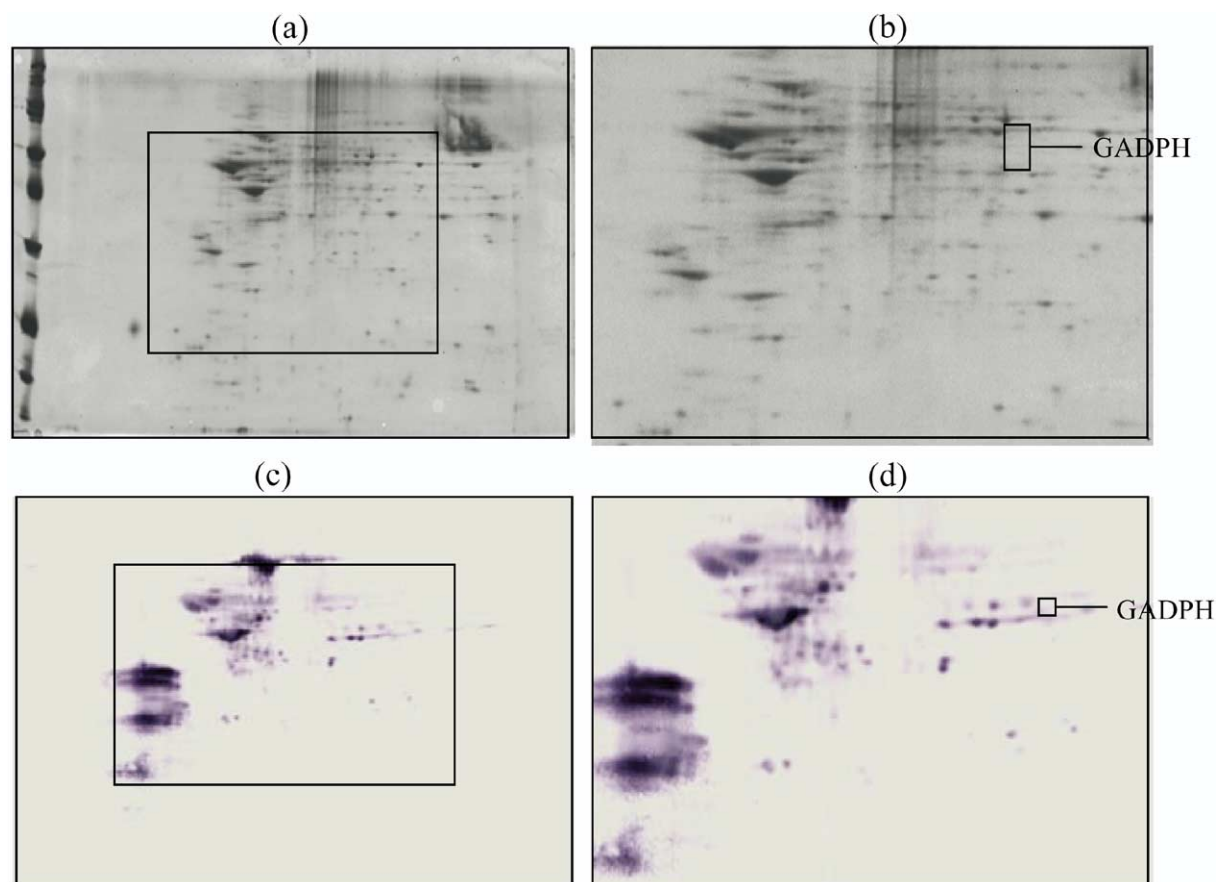


**Fig. 8.** 2D gel (a, b) and blot (c, d) from the sample immunoprecipitated with anti-GADPH antibody. Box represents the enlargements of 2D gel and blot.

taining hyperphosphorylated tau. Tau is a microtubule-associated protein that when hyperphosphorylated is thought to disassociate from microtubules resulting in microtubule instability and neurodegeneration. Moreover, 14-3-3  $\zeta$  has been shown to act as an effector of tau protein phosphorylation (Hashiguchi et al., 2000) and many act as a scaffolding protein to promote the polymerization of tau protein (Hernández et al., 2004). Recently, it has been shown that 14-3-3  $\zeta$  acts as a scaffolding protein simultaneously binding to tau and glycogen synthase kinase 3 $\beta$  (GSK3 $\beta$ ) in a multiprotein tau phosphorylation complex (Agarwal-Mawal et al., 2003). GSK3 $\beta$  has been shown to be one of the kinases involved in the hyperphosphorylation of tau (Grimes and Jope, 2001). Based on the different regulatory mechanisms exerted by 14-3-3 on its target proteins, it has been proposed that 14-3-3 binding may alter the conformation of tau making it more susceptible to phosphorylation (Hashiguchi et al., 2000). Additionally, binding of 14-3-3 may protect the hyperphosphorylated form of tau from dephosphorylation promoting the formation of NFTs and possibly preventing the complex from proteolysis (Agarwal-Mawal et al., 2003).

In this study, we found 14-3-3  $\zeta$  to be significantly oxidized in both the NBM and the hippocampus of rats injected with A $\beta$ (1–42). It is feasible that A $\beta$ (1–42)-induced oxidation of 14-3-3  $\zeta$  could change the conformation

of the protein in such a way as to facilitate its binding of GSK3 $\beta$  and tau. Moreover, 14-3-3  $\zeta$  may increase the kinase activity of GSK3 $\beta$  promoting the hyperphosphorylation of tau leading to the formation of NFTs and further neurodegeneration as detected in AD. Although there is no evidence of tau neurofilaments in brains of rats injected with A $\beta$ (1–42), it is conceivable that the above considerations may support the notion that A $\beta$ (1–42)-mediated processes create the conditions for formation of NFTs, i.e. support the idea that A $\beta$ (1–42) deposition precedes and is responsible for tangle formation in AD brain.

In this study, we found a number of metabolic enzymes to be oxidized by A $\beta$ (1–42), consistent with altered energy metabolism in AD (Vanhanen and Soininen, 1998; Scheltens and Korf, 2000; Messier and Gagnon, 2000). These enzymes include glyceraldehyde-3-phosphate dehydrogenase, pyruvate dehydrogenase (lipoamide dehydrogenase), and phosphoglycerate mutase 1. Glyceraldehyde-3-phosphate dehydrogenase is a glycolytic enzyme located in the cytosol that catalyzes the conversion of glyceraldehyde-3-phosphate to 1,3-phosphoglycerate. Accumulation of this enzyme along with  $\alpha$ -enolase and  $\gamma$ -enolase has been shown in AD brain (Schonberger et al., 2001). Additionally, reduced activity of glyceraldehyde-3-phosphate dehydrogenase has been reported in AD (Mazzola and Sirover, 2001). Oxidation and subsequent



loss of function of glyceraldehyde-3-phosphate dehydrogenase could result in decreased ATP production, a finding consistent with the altered glucose tolerance and metabolism confirmed by PET scanning studies of AD patients (Vanhanen and Soininen, 1998; Messier and Gagnon, 2000; Blass and Gibson, 1991; Scheltens and Korf, 2000; Ogawa et al., 1996).

Pyruvate dehydrogenase is a mitochondrial multienzyme complex that involves five cofactors and catalyzes the oxidative decarboxylation of pyruvate to acetyl CoA, the key step where the product of glycolysis feeds into the citric acid cycle. Previous studies have shown that acrolein, a reactive alkenal product of lipid peroxidation similar to HNE and elevated in AD brain (Lovell et al., 2001), has been shown to bind to and decrease the activity of pyruvate dehydrogenase (Pocernich and Butterfield, 2003). Therefore, it is likely that the oxidation of pyruvate dehydrogenase by A $\beta$ (1–42) would result in the loss of function of this enzyme contributing to altered glucose metabolism and loss of production of ATP. Indeed, decreased activity of pyruvate dehydrogenase has been reported in AD (Gibson et al., 1988). It is important to note that in this study we found the lipoamide component of the multienzyme complex to be oxidized which is a FAD dependent enzyme that is responsible for the transfer of the acetyl group from lipoic acid to coenzyme A coupled with the oxidation of lipoic acid and the reduction of NAD<sup>+</sup>. Thus, the formation of acetyl CoA itself may be prevented by the loss of function of the lipoamide form of pyruvate dehydrogenase. This is supported by the increase in pyruvate and lactate reported in CSF of AD patients (Parnetti et al., 1995, 2000). Also related to cholinergic dysfunction in AD, A $\beta$ (1–42) injection into rat brain led to a reversible decrease in the number of choline acetyltransferase (ChAT)-positive neurons, but also a decrease in extracellular acetylcholine levels (Giovannelli et al., 1998). A $\beta$ (1–42) addition to ChAT-containing synaptosomal preparations led to elevated covalent modification of this enzyme by 4-hydroxy-2-*trans*-nonenal, a product of lipid peroxidation (Butterfield and Lauderback, 2002).

Two proteins found to be significantly oxidized in the hippocampus by A $\beta$ (1–42) were identified as phosphoglycerate mutase 1. The two proteins were resolved as individual protein spots in the 2D-gels and 2D-oxyblots used in this study. The spots were present as a “train” of proteins and were similar in molecular migration, but varied in pI suggesting the possibility that the two spots represent different phosphorylation states of phosphoglycerate mutase 1. Nevertheless, it is important to note that both forms of phosphoglycerate mutase 1 were found to be significantly oxidized. Additionally, decreased expression of phosphoglycerate mutase 1 has been reported in AD (Iwangoff et al., 1980). Phosphoglycerate mutase 1 is activated by 2,3-bisphosphoglycerate and catalyzes the interconversion of 3- and 2-phosphoglycerate in the steps leading to the production of the second equivalent of ATP in glycolysis. Loss of function of phosphoglycerate mutase 1 is consistent with altered glucose metabolism in AD (Ogawa et al., 1996) and could lead to the accumulation of

glycolytic intermediates, decreased production of pyruvate, and consequently, decreased production and availability of ATP. Lack of ATP would consequently lead to dysfunction in ion pumps, electrochemical gradients, voltage-gated ion channels, and cell potential, all of which are needed to combat the oxidative stress of synaptic regions of neurons induced by A $\beta$ (1–42).

Also in this study, GS was identified as a target of A $\beta$ (1–42)-induced protein oxidation. This finding is consistent with the oxidation and decreased activity of GS in AD brain (Castegna et al., 2002a; Hensley et al., 1995). Our findings are particularly important as they provide supporting evidence for the role of A $\beta$ (1–42) as a mediator of oxidative stress in AD brain. GS is an enzyme that catalyzes the conversion of glutamate to glutamine. Loss of function of GS would result in the decreased conversion of glutamate leading to the extracellular accumulation of glutamate. Excess glutamate would stimulate NMDA receptors leading to excitotoxicity and neuronal death, two factors that could play an important role in neurodegeneration and AD (Casamenti et al., 1999).

$\beta$ -Tubulin has been shown to exhibit a non-significant trend toward oxidation in AD brain (Aksenov et al., 2001). In this study, a protein spot that exhibited a significant increase in protein oxidation was identified as a mixture of tubulin  $\beta$  chain 15 and  $\alpha$ -tubulin. Due to the similarities in molecular weight and pI we are unable to distinguish between the two proteins at this time. Tubulin is a core protein of microtubules, which play a role in cytoskeletal maintenance. Additionally, tubulin has been shown to be involved in the transport of membrane-bound organelles and is required for extension and maintenance of neurites. The oxidation of tubulin leading to loss of protein function could result in loss of neuronal connections and communication, as well as compromised cellular structure which would play important roles in neurodegeneration.

$\alpha$ -Synuclein is a presynaptic protein that normally plays a role in synaptic vesicle homeostasis, but accumulates in filaments in diseases associated with Lewy bodies, such as Parkinson's disease and AD. In rat brain,  $\alpha$ -synuclein has been shown to play a role in catecholaminergic components of the CNS, while  $\beta$ -synuclein is associated with cholinergic components particularly in the basal forebrain (Li et al., 2002). In the current study, we found  $\beta$ -synuclein to be significantly oxidized by A $\beta$ (1–42). The function of  $\beta$ -synuclein is unknown, but human  $\beta$ -synuclein has a 62% amino acid sequence homology with  $\alpha$ -synuclein and both proteins are concentrated in nerve terminal suggesting that the two may play similar roles in synapse formation in the brain (Nakajo et al., 1993). If  $\beta$ -synuclein is involved in synapse formation in cholinergic regions of the brain, loss of function due to oxidation could result in loss of synapses and cholinergic deficits documented in AD (Masliah et al., 1994; Frölich, 2002; Giovannini et al., 2002). Recently,  $\beta$ -synuclein has been shown to increase Akt activity by direct interaction with Akt in neuroblastoma cells transfected with  $\beta$ -synuclein. The increase in Akt activity was shown to protect against rotenone, suggesting that  $\beta$ -synuclein may

play a protective role in the CNS (Hashimoto et al., 2004). If this is the case, oxidation of  $\beta$ -synuclein could lead to a conformation change in the protein preventing its direct interaction with Akt and abolishing this protective effect.

Chaperonin 60 (Cpn60), or heat shock protein 60 (HSP60), is a mitochondrial chaperone protein that is involved in mediating the proper folding and assembly of mitochondrial proteins, especially in response to oxidative stress (Bozner et al., 2002). Additionally, HSP60 has been proposed to play a role as an anti-apoptotic protein (Lin et al., 2001). Expression of HSP60 is significantly decreased in AD (Yoo et al., 2001) and  $A\beta$ (25–35) has been shown to induce oxidation of HSP60 in fibroblasts derived from AD patients compared with age matched controls (Choi et al., 2003). We found HSP60 to be significantly oxidized by  $A\beta$ (1–42). The loss of function of HSP60 could lead to increased protein misfolding and aggregation, as well as an increased vulnerability to oxidative stress. This is particularly important due to the lack of mechanisms to protect mitochondrial from oxidative stress and the vicinity of mitochondrial proteins to reactive oxygen species generated during normal oxidative phosphorylation and more so in concert with mitochondrial dysfunction.

To confirm the correct identification of the reported oxidized proteins we used two different approaches. We selected 14-3-3  $\zeta$  and GADPH as example proteins. The specificity of 14-3-3  $\zeta$  was confirmed by probing the Western blots with anti-14-3-3  $\zeta$  antibody and comparing its position on a ponceau-stained blot and that of the total oxidized proteins (Fig. 7). Based on this method we found 14-3-3  $\zeta$  at the same position on the gel as reported in for that from hippocampus. In addition, immunoprecipitation of the GADPH protein by anti-GADPH showed the absence of protein spot corresponding to GADPH in the respective gel and blot (Fig. 8). Taken together, both these experiments confirmed the correct identification of the reported proteins in the present study.

In summary, we evaluated the regional effects of protein oxidation induced by  $A\beta$ (1–42) injected into rat brain. We identified eight proteins to be significantly oxidized: 14-3-3  $\zeta$ , HSP60, GS, tubulin  $\beta$  chain 15/ $\alpha$ -tubulin,  $\beta$ -synuclein, glyceraldehyde-3-phosphate dehydrogenase, pyruvate dehydrogenase, and phosphoglycerate mutase 1. Loss of function, or altered function, of these proteins due to conformation changes induced by oxidation could lead to the NFT pathology, increased protein aggregation, excitotoxicity, loss of cytoskeletal integrity, loss of synapse and neuronal communication, and altered energy metabolism all of which are associated with AD. More importantly, however, this work supports the role of  $A\beta$ (1–42) as a mediator of oxidative stress and its implication in the pathogenesis of AD.

This study has shown that a single injection of  $A\beta$ (1–42) in the NBM is sufficient to modify a number of proteins not only in the NBM around the injection site, but also in other brain regions, in this case, the cortex and hippocampus. Moreover, these oxidatively modified proteins are in some cases similar to those found in AD brain or implicated in pathways known to be defective in this disorder,

e.g. excitotoxicity, metabolism, oxidative stress, protein aggregation, cholinergic dysfunction, etc. (Butterfield and Lauderback, 2002; Butterfield, 2004). Therefore, we posit that our results confirm that the injection of  $A\beta$ (1–42) is a good model for investigating pathogenic mechanisms of AD, and that  $A\beta$ (1–42) is directly or indirectly responsible for the oxidative changes observed in rat brains and AD brain. It is possible that downstream effects of  $A\beta$ (1–42)-induced lipid peroxidation products [e.g. oxidative modification of proteins by HNE (Butterfield et al., 2002; Lauderback et al., 2001)] and neuroinflammation (Giovannini et al., 2002) contribute indirectly to the  $A\beta$ (1–42)-induced changes reported here.

*Acknowledgments*—This work was supported in part by NIH grants to D.A.B. [AG-05119; AG-10836] and by a grant from Cassa di Risparmio di Firenze to F.C.

## REFERENCES

- Agarwal-Mawal A, Qureshi HY, Cafferty PW, Yuan Z, Han D, Lin R, Paudel HK (2003) 14-3-3 Connects glycogen synthase kinase-3 beta to tau within a brain microtubule-associated tau phosphorylation complex. *J Biol Chem* 278:12722–12728.
- Aksenov MY, Aksenova MV, Butterfield DA, Geddes JW, Markesbery WR (2001) Protein oxidation in the brain in Alzheimer's disease. *Neuroscience* 103:373–383.
- Aksenov MY, Tucker HM, Nair P, Aksenova MV, Butterfield DA, Estus S, Markesbery WR (1999) The expression of several mitochondrial and nuclear genes encoding the subunits of electron transport chain enzyme complexes, cytochrome c oxidase, and NADH dehydrogenase in different brain regions in Alzheimer's disease brain. *Neurochem Res* 24:767–774.
- Blass JP, Gibson GE (1991) The role of oxidative abnormalities in the pathophysiology of Alzheimer's disease. *Rev Neurol* 147:513–525.
- Bozner P, Wilson GL, Druzhyna NM, Bryant-Thomas TK, LeDoux SP, Wilson GL, Pappolla MA (2002) Deficiency of chaperonin 60 in Down's syndrome. *J Alzheimers Dis* 4:479–486.
- Burkhard PR, Sanchez JC, Landis T, Hochstrasser DF (2001) CSF detection of the 14-3-3 protein in unselected patients with dementia. *Neurology* 56:1528–1533.
- Butterfield DA (2002) Amyloid beta-peptide (1–42)-induced oxidative stress and neurotoxicity: implications for neurodegeneration in Alzheimer's disease brain. *Free Radic Res* 36:1307–1313.
- Butterfield DA (2003) Amyloid beta-peptide [1–42]-associated free radical-induced oxidative stress and neurodegeneration in Alzheimer's disease brain: mechanisms and consequences. *Curr Med Chem* 10:2651–2659.
- Butterfield DA (2004) Proteomics: a new approach to study oxidative stress in Alzheimer's disease brain. *Brain Res* 1000:1–7.
- Butterfield DA, Drake J, Pocernich C, Castegna A (2001) Evidence of oxidative damage in Alzheimer's disease brain: central role for amyloid beta-peptide. *Trends Mol Med* 7:548–554.
- Butterfield DA, Lauderback CM (2002) Lipid peroxidation and protein oxidation in Alzheimer's disease brain: potential causes and consequences involving amyloid beta-peptide-associated free radical oxidative stress. *Free Rad Biol Med* 32:1050–1060.
- Butterfield DA, Stadtman ER (1997) Protein oxidation processes in aging brain. *Adv Cell Aging Gerontol* 2:161–191.
- Casamenti F, Prosperi C, Scali C, Giovannelli L, Colivicchi MA, Fausone-Pelligrini MS, Pepeu G (1999) Interleukin-1  $\beta$  activates forebrain glial cells and increases nitric oxide production and cortical glutamate and GABA release in vivo: implication for Alzheimer's disease. *Neuroscience* 91:831–842.
- Castegna A, Aksenov M, Aksenova M, Thongboonkerd V, Klein JB, Pierce WM, Booze R, Markesbery WR, Butterfield DA (2002a) Pro-

- teomic identification of oxidatively modified proteins in Alzheimer's disease brain part I: creatine kinase BB, glutamine synthetase, and ubiquitin carboxy-terminal hydrolase L-1. *Free Rad Biol Med* 33:562–571.
- Castegna A, Aksenov M, Thongboonkerd, Klein JB, Pierce WM, Booze R, Markesbery WR, Butterfield DA (2002b) Proteomic identification of oxidatively modified proteins in Alzheimer's disease brain: Part II. Dihydropyrimidinase-related protein 2,  $\alpha$ -enolase, and heat shock cognate 71. *J Neurochem* 82:1524–1532.
- Castegna A, Thongboonkerd V, Klein J, Lynn BC, Wang YL, Osaka H, Wada K, Butterfield DA (2004) Proteomic analysis of brain proteins in the gracile axonal dystrophy (gad) mouse, a syndrome that emanates from dysfunctional ubiquitin carboxyl-terminal hydrolase L-1, reveals oxidation of key proteins. *J Neurochem* 88:1540–1546.
- Castegna A, Thongboonkerd V, Klein JB, Lynn B, Markesbery WR, Butterfield DA (2003) Proteomic identification of nitrated proteins in Alzheimer's disease brain. *J Neurochem* 85:1394–1401.
- Choi J, Levey AI, Weintraub ST, Rees HD, Gearing M, Chin L-S, Li L (2004) Oxidative modifications and down regulation of ubiquitin carboxyl-terminal hydrolase L1 associated with idiopathic Parkinson's and Alzheimer's diseases. *J Biol Chem* 279:13256–13264.
- Choi J, Malakowsky CA, Talent JM, Conrad CC, Carrl CA, Weintraub ST, Gracy RW (2003) Anti-apoptotic proteins are oxidized y Ab25–35 in Alzheimer's fibroblasts. *Biochim Biophys Acta* 1637:135–141.
- Dougherty MK, Morrison DK (2004) Unlocking the code of 14-3-3. *J Cell Sci* 117:1875–1884.
- Drake J, Link CD, Butterfield DA (2003) Oxidative stress precedes fibrillar deposition of Alzheimer's disease amyloid  $\beta$ -peptide (1–42) in a transgenic *Caenorhabditis elegans* model. *Neurobiol Aging* 24:415–420.
- Esterbauer H, Schaur RJ, Zollner H (1991) Chemistry and biochemistry of 4-hydroxynonenal, malonaldehyde and related aldehydes. *Free Rad Biol Med* 11:81–128.
- Fountoulakis M, Cairns N, Lubec G (1999) Increased levels of 14-3-3 gamma and epsilon proteins in brain of patients with Alzheimer's disease and Down syndrome. *J Neural Transm Suppl* 57:323–335.
- Frautschy SA, Baird A, Cole GM (1991) Effects of injection of Alzheimer  $\beta$ -amyloid cores in rat brain. *Proc Natl Acad Sci USA* 88:8362–8366.
- Frölich L (2002) The cholinergic pathology in Alzheimer's disease: discrepancies between clinical experience and pathophysiological findings. *J Neural Transm* 109:1003–1014.
- Gibson GE, Sheu KF, Blass JP, Baker A, Carlson KC, Harding B, Perrino P (1988) Reduced activities of thiamine-dependent enzymes in the brains and peripheral tissues of patients with Alzheimer's disease. *Arch Neurol* 45:836–840.
- Giovannelli L, Scali C, Faussone-Pelligrini MS, Pepeu G, Casamenti F (1998) Long-term changes in the aggregation state and toxic effects of  $\beta$ -amyloid injected into the rat brain. *Neuroscience* 87:349–357.
- Giovannini MG, Scali C, Prosperi C, Bellucci A, Vannucchi MG, Rosi S, Pepeu G, Casamenti F (2002)  $\beta$ -amyloid-induced inflammation and cholinergic hypofunction in the rat brain *in vivo*: involvement of the p38MAPK pathway. *Neurobiol Dis* 11:257–274.
- Grimes CA, Joep RS (2001) The multifaceted roles of glycogen synthase kinase 3beta in cellular signaling. *Prog Neurobiol* 65:391–426.
- Hashiguchi M, Sobue K, Paudel HK (2000) 14-3-3 Zeta is an effector of tau protein phosphorylation. *J Biol Chem* 275:25247–25254.
- Hashimoto M, Baron P, Ho G, Takenouchi T, Rockenstein E, Crews L, Masliah E (2004)  $\beta$ -Synuclein regulated Akt activity in neuronal cells: a possible mechanism for neuroprotection in Parkinson's disease. *J Biol Chem*, published online March 16, 2004.
- Hensley K, Hall N, Subramaniam R, Cole P, Harris M, Aksenov M, Aksenova M, Gabbita P, Wu JF, Carney JM, Lovell M, Markesbery WR, Butterfield DA (1995) Brain regional correspondence between Alzheimer's disease histopathology and biomarkers of protein oxidation. *J Neurochem* 65:2146–2156.
- Hernández F, Cuadros R, Avila J (2004) Zeta 14-3-3 protein favours the formation of human tau fibrillar polymers. *Neurosci Lett* 357:143–146.
- Iwangoff P, Armbruster R, Enz A, Meier-Ruge W (1980) Glycolytic enzymes from human autaptic brain cortex: normal aged and demented cases. *Mech Ageing Dev* 14:203–209.
- Lauderback CM, Hackett JM, Huang FF, Keller JN, Szveda LI, Markesbery WR, Butterfield DA (2001) The glial glutamate transporter, GLT-1, is oxidatively modified by 4-hydroxy-2-nonenal in the Alzheimer's disease brain: the role of Abeta 1–42. *J Neurochem* 78:413–416.
- Layfield R, Fergusson J, Aitken A, Lowe J, Landon M, Mayer RJ (1996) Neurofibrillary tangles of Alzheimer's disease brains contain 14-3-3 proteins. *Neurosci Lett* 209:57–60.
- Levine RL, Williams JA, Stadtman ER, Shacter E (1994) Carbonyl assays for determination of oxidatively modified proteins. *Methods Enzymol* 233:346–357.
- Li JY, Henning Jensen P, Dahlstrom A (2002) Differential localization of  $\alpha$ -,  $\beta$ -, and  $\gamma$ -synucleins in the rat CNS. *Neuroscience* 113:463–478.
- Lin KM, Lin B, Lian IY, Mestrl R, Scheffler IE, Dillmann WH (2001) Combined and individual mitochondrial HSP60 and HSP10 expression in cardiac myocytes protects mitochondrial function and prevents apoptotic cell deaths induced by simulated ischemia-reoxygenation. *Circulation* 103:1787–1792.
- Lovell MA, Xie C, Markesbery WR (2001) Acrolein is increased in Alzheimer's disease brain and is toxic to primary hippocampal cultures. *Neurobiol Aging* 22:187–194.
- Mark RJ, Lovell MA, Markesbery WR, Uchida K, Mattson MP (1997) A role for 4-hydroxynonenal, an aldehydic product of lipid peroxidation, in disruption of ion homeostasis and neuronal death induced by amyloid beta-peptide. *J Neurochem* 68:255–264.
- Markesbery WR, Lovell MA (1998) Four-hydroxynonenal, a product of lipid peroxidation, is increased in the brain in Alzheimer's disease. *Neurobiol Aging* 19:33–36.
- Masliah E, Alford M, DeTeresa R, Mallory M, Hansen L (1996) Deficient glutamate transport is associated with neurodegeneration in Alzheimer's disease. *Ann Neurol* 40:759–766.
- Masliah E, Mallory M, Hansen L, De Teresa R, Alford M, Terry R (1994) Synaptic and neuritic alterations during the progression of Alzheimer's disease. *Neurosci Lett* 174:67–72.
- Mazzola JL, Sirover MA (2001) Reduction of glyceraldehydes-3-phosphate dehydrogenase activity in Alzheimer's disease and in Huntington's disease fibroblasts. *J Neurochem* 76:442–449.
- Messier C, Gagnon M (2000) Glucose regulation and brain aging. *J Nutr Health Aging* 4:208–213.
- Mohammad-Abdul H, Wenk GL, Grammling M, Hauss-Wegrzyniak B, Butterfield DA (2004) APP and PS-1 mutations induce brain oxidative stress independent of dietary cholesterol. *Neurosci Letts* 368:148–150.
- Nakajo S, Tsukada K, Omata K, Nakamura K (1993) A new brain-specific 14 kd protein is a phosphoprotein: its complete amino acid sequence and evidence for phosphorylation. *Eur J Biochem* 217:1057–1063.
- Ogawa M, Fukuyama H, Ouchi Y, Yamauchi H, Kimura J (1996) Altered energy metabolism in Alzheimer's disease. *J Neurol Sci* 139:78–82.
- Parnetti L, Gaiti A, Polidori MC, Brunetti M, Palumbo B, Chionne F, Cadini D, Checchetti R, Senin U (1995) Increased cerebrospinal fluid pyruvate levels in Alzheimer's disease. *Neurosci Lett* 199:231–233.
- Parnetti L, Reboldi GP, Gallai V (2000) Cerebrospinal fluid pyruvate levels in Alzheimer's disease and vascular dementia. *Neurology* 54:735–737.
- Paxinos G, Watson C (1998) The rat brain in stereotaxic coordinates. New York: Academic Press.

- Pocernich CB, Butterfield DA (2003) Acrolien inhibits NADH-linked mitochondrial enzyme activity: implications for Alzheimer's disease. *Neurotox Res* 5:515–520.
- Scheltens P, Korf ESC (2000) Contribution of neuroimaging in the diagnosis of Alzheimer's disease and other dementias. *Curr Opin Neurol* 13:391–396.
- Schonberger SJ, Edgar PF, Kydd R, Faull RLM, Cooper GJS (2001) Proteomic analysis of the brain in Alzheimer's disease: molecular phenotype of a complex disease process. *Proteomics* 1:1519–1528.
- Selkoe DJ (2001) Alzheimer's disease results from the cerebral accumulation and cytotoxicity of amyloid beta-protein. *J Alzheimers Dis* 3:75–80.
- Subramaniam R, Roediger F, Jordan B, Mattson MP, Keller JN, Waeg G, Butterfield DA (1997) The lipid peroxidation product, 4-hydroxy-2-trans-nonenal, alters the conformation of cortical synaptosomal membrane protein. *J Neurochem* 69:1161–1169.
- Takahashi Y (2003) The 14-3-3 proteins: gene, gene expression, and function. *Neurochem Res* 28:1265–1273.
- Thongboonkerd V, Luengpailin J, Cao J, Pierce QM, Cai J, Klein JB, Doyle RJ (2002) Fluoride exposure attenuates expression of *Streptococcus pyrogenes* virulence factors. *J Biol Chem* 277:16599–16605.
- Vanhanen M, Soininen H (1998) Glucose intolerance, cognitive impairment and Alzheimer's disease. *Curr Opin Neurol* 11:673–677.
- Varadarajan S, Yatin S, Aksenova M, Butterfield DA (2000) Review: Alzheimer's amyloid beta-peptide-associated free radical oxidative stress and neurotoxicity. *J Struct Biol* 130:184–208.
- Whitehouse PJ, Price DL, Clark AW, Coyle JT, DeLong MR (1981) Alzheimer's disease: evidence for selective loss of cholinergic neurons in the nucleus basalis. *Ann Neurol* 10:122–126.
- Yatin SM, Varadarajan S, Link CD, Butterfield DA (1999) In vitro and in vivo oxidative stress associated with Alzheimer's amyloid  $\beta$ -peptide (1–42). *Neurobiol Aging* 20:325–330.
- Yatin SM, Varadarajan S, Butterfield DA (2000) Vitamin E prevents Alzheimer's amyloid beta-peptide (1–42)-induced protein oxidation and reactive oxygen species formation. *J Alzheimer's Dis* 2:123–131.
- Yoo BC, Kim SH, Cairns N, Fountoulakis M, Lubec G (2001) Deranged expression of molecular chaperones in brains of patients with Alzheimer's disease. *Biochem Biophys Res Commun* 280:249–258.

(Accepted 12 December 2004)  
(Available online 10 March 2005)